Environmental Science & Technology

Article

Cite This: Environ. Sci. Technol. XXXX, XXX, XXX−XXX

pubs.acs.org/est

Detailed Speciation of Intermediate Volatility and Semivolatile Organic Compound Emissions from Gasoline Vehicles: Effects of Cold-Starts and Implications for Secondary Organic Aerosol Formation

Greg T. Drozd,[†,*] Yunliang Zhao,[§] Georges Saliba,[§] Bruce Frodin,[∥] Christine Maddox,[∥] M.-C. Oliver Chang,[∥] Hector Maldonado,[∥] Satya Sardar,[∥] Robert Jay Weber,[‡] Allen L. Robinson,[§] and Allen H. Goldstein[‡]

[†]Department of Chemistry, Colby College, Waterville, Maine 04901, United States

[‡]Department of Environmental Science, Policy, and Management, University of California, Berkeley, California 94720, United States

[§]Center for Atmospheric Particle Studies, Carnegie Mellon University, Pittsburgh, Pennsylvania 15213, United States

[∥]California Air Resources Board, Sacramento, California 95814, United States

Supporting Information

ABSTRACT: Over the past two decades vehicle emission standards in the United States have been dramatically tightened with the goal of reducing urban air pollution. Secondary organic aerosol (SOA) is the dominant contributor to urban organic aerosol. Experiments were conducted at the California Air Resources Board Haagen-Smit Laboratory to characterize exhaust organics from 20 gasoline vehicles recruited from the California in-use fleet. The vehicles spanned a wide range of emission certification standards. We comprehensively characterized intermediate volatility and semivolatile organic compound emissions using thermal desorption two-dimensional gas-chromatography−mass-spectrometry with electron impact (GC × GC-EI-MS) and vacuum-ultraviolet (GC × GC-VUV-MS) ionization. Single-ring aromatic compounds with unsaturated C4 and C5 substituents contribute a large fraction of the intermediate volatility organic compound (IVOC) emissions in gasoline vehicle exhaust. The analyses of quartz filters used in GC × GC-VUV-MS show that primary organic aerosol emissions were dominated by motor oil. We combined our new emissions data with published SOA yield parametrizations to estimate SOA formation potential. After 24 h of oxidation, IVOC emissions contributed 45% of SOA formation; BTEX compounds (benzene, toluene, xylenes, and ethylbenzene), 40%; other VOC aromatics, 15%. The composition of IVOC emissions was consistent across the test fleet, suggesting that future reductions in vehicular emissions will continue to reduce SOA formation and ambient particulate mass levels.

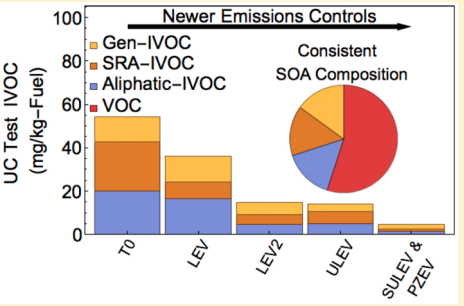

INTRODUCTION

Tailpipe emissions of nonmethane organic gases (NMOG) from gasoline vehicles contribute significantly to secondary organic aerosol (SOA) formation in urban areas.[1−8] Important classes of SOA precursors identified in NMOG emitted from gasoline vehicles include small, single-ring aromatics (e.g., toluene); intermediate volatility organic compounds (IVOC); and semivolatile organic compounds (SVOC).[9−13] IVOCs have recently been estimated to contribute up to half of all SOA formation from gasoline vehicle exhaust, changing the view that small, single ring aromatics alone dominate formation of SOA from gasoline vehicles.[10,12,14−17]

Vehicle organic emissions span a broad range of volatilities, and their composition depends on the engine inputs (fuel and oil), processing (combustion and aftertreatment), engine operations (e.g., cold-start versus hot stabilized), and emission control technologies (e.g., catalysts). Volatility is commonly categorized using effective saturation concentration (C^*), with volatility increasing for higher C^*. Volatile organic compound (VOC) emissions ($C^* > 10^6$ $\mu g\ m^{-3}$), which make up the majority of total NMOG emissions from gasoline vehicles, are mainly attributed to unburned fuel, combustion products, and degradation products formed in the aftertreatment system.[4,12,18−21] IVOC emissions ($10^3 < C^* < 10^6$ $\mu g\ m^{-3}$) likely have similar sources; this is supported by strong correlations between IVOC and total NMOG.[22,23] SVOC emissions are mainly derived from engine oil; a portion of these are emitted as fine particulate matter (PM) due to their lower volatility.[20,24,25] Predicting SOA formation from on-road gasoline vehicles thus requires an understanding of the

Received: October 4, 2018
Revised: December 23, 2018
Accepted: December 25, 2018
Published: December 25, 2018

DOI: 10.1021/acs.est.8b05600
Environ. Sci. Technol. XXXX, XXX, XXX−XXX

emissions of all of these classes of organics and their dependence on engine operations.

A challenge is that IVOC and SVOC emissions are composed of hundreds and potentially thousands of individual compounds and therefore have not generally been characterized at the molecular level, leaving a large unresolved complex mixture.[26] Instead, they are typically reported as broad groups such as aliphatic, cyclic, aromatic, and branched compounds.[22−24] More detailed structural information such as the type of branching, number of substituents, and type of substituents (linear vs iso) is not known for all volatility ranges.[5] Differences in molecular structure can influence SOA formation from oxidation in the atmosphere.[14,27] The accurate prediction of current and future SOA formation from vehicle emissions requires this level of detailed compositional information for a wide range of vehicle types.

Over the last several decades, regulations have been implemented to reduce ozone, nitrogen oxides (NO + NO_2 = NO_x), and PM levels in the United States. Regulations to control ambient ozone have led to dramatic reductions in vehicular NMOG emissions. SOA precursors that contribute a significant fraction of ambient fine particulate matter are a subset of the NMOG emissions.[28−30] Therefore, the reduction of NMOG emissions from gasoline vehicles has a secondary benefit of reductions in SOA formation and ambient PM.[4,13,31] However, current emission regulations limit total NMOG and a few specific toxic species as opposed to SOA precursors. Therefore, questions remain with respect to the effectiveness of emission controls for reducing SOA formation.[32] In addition to the molecular structure of organic compound emissions, SOA formation also depends on ambient NO_x levels.[7,13,33] Future reductions in SOA formation will thus depend on both reductions in total NMOG emissions and any changes in the composition of these emissions.

Past smog experiments that photo oxidized diluted vehicle exhaust have shown that less SOA is formed from newer, lower NMOG-emitting gasoline vehicles that meet more stringent emission standards than that from older, higher emitting vehicles.[4,11,32,34] However, in some cases, this reduction in SOA is less than proportional to the reduction in NMOG emissions, suggesting that the yield of SOA per mass of NMOG has increased for newer vehicles.[10,11,35] One potential explanation is that newer aftertreatment technologies are less effective at removing effective SOA precursors than other classes of compounds. Recent work has shown enrichment in SOA-forming IVOC emissions for newer vehicles.[15] If aftertreatment creates a more potent mix of precursors that leads to higher yields of SOA despite a lower mass of emissions, then future reductions in NMOG emissions may have a lesser cobenefit of reducing SOA formation and total ambient PM. However, the work also suggests that the apparent increase in SOA formation in chamber oxidation studies can be due to changes in NO_x levels affecting SOA yields rather than changes in NMOG composition.[13]

We performed comprehensive measurements to characterize gasoline vehicle NMOG emissions across a wide range of volatility. Here, we focus on the IVOC and SVOC emissions measured during chassis dynamometer testing of gasoline vehicles recruited from the Southern California in-use fleet to determine the effects of control technologies and engine state (cold-start vs hot-running and hot-start) on the magnitude and speciation of the emissions. We used state-of-the-art GC techniques to classify characteristics that determine SOA formation (volatility and chemical structure).[36,37] These techniques allowed a much higher degree of characterization than previous work.

EXPERIMENTAL METHODS

Fleet Overview. The test fleet included 20 light duty gasoline vehicles recruited from southern California rental agencies, the Air Resources Board vehicle pool, and southern California residents. The vehicles spanned model years from 1990 to 2014 and therefore featured a range of engine and emission control technologies. The vehicle fleet was chosen to examine the effectiveness of the newest emission control systems while including older vehicles to provide context and continuity with previous studies. Vehicles are classified by their emissions certification standard. The test fleet included: one Tier 0 vehicle (T0), one low emission vehicle (LEV I), two Tier 2 low emission vehicles (LEV II) vehicles, five ultralow emission vehicles (ULEV), five superultra-low emission vehicles (SULEV), and six partial-zero emission vehicles (PZEV). Because the PZEV and SULEV vehicles have the same tailpipe emission standards, results from these are combined and termed SULEV. It should be noted that our vehicle fleet was dominated by newer vehicles that met stringent emission standards, and our highest emitting vehicle (tier 0) had lower than average IVOC emissions compared to previous studies.[10,22,30] A complete list of vehicles with descriptions and traditional emissions data are presented in Saliba et al. and Drozd et al.[21,38]

Dynamometer Tests. All vehicles were tested on a chassis dynamometer using the standard cold-start unified cycle (UC) driving protocol at the California Air Resources Board (ARB) Haagen-Smit Laboratory. The UC protocol consists of three operating phases: cold-start, hot-stabilized, and hot-start. The UC protocol is similar in overall duration and distance to the Federal Test Procedure (FTP), but it was developed specifically to represent driving in Southern California. It has more aggressive driving with harder acceleration periods than the FTP, which results in higher emissions.[4] While the FTP protocol is used to certify emission standards for both the ARB and US EPA, the same trends in emissions due to changes in vehicle technology are expected for either drive protocol. The UC protocol has been used for emission inventory development. Recent work has also used the UC protocol to characterize IVOC emissions, allowing for more direct comparison in trends of emissions across studies and test fleets.[4,10,39] Prior to cold-start tests, vehicles were conditioned with an overnight soak. Tailpipe emissions were sampled directly into a constant volume sampler (CVS) that diluted the exhaust by a factor of 10−30. All vehicles were tested using the same commercial summertime gasoline provided by ARB; details on composition are published in a companion paper.[21]

Sampling and Analysis of VOC, IVOC, and SVOC. VOC, IVOC, SVOC, and PM were sampled similarly to previous studies.[4,22] This work focuses only on the primary organic aerosol (POA) fraction of the PM. Dilute emissions were sampled directly off the end of the CVS through a heated (47 °C) silicosteel treated transfer line. The transfer line was ∼5 m long. Samples were then collected using two sample trains. This setup is shown in Figure S1. The first train consisted of a quartz filter (Q1) followed by a second quartz filter (Q2) in series (47 mm, Pall-Gelman, Tissuquartz 2500 QAOUP). The second train consisted of a Teflon filter (TF, 47 mm, Pall-Gelman, Teflo R2PJ047) followed by two parallel

DOI: 10.1021/acs.est.8b05600
Environ. Sci. Technol. XXXX, XXX, XXX−XXX

sets of Tenax-TA sorbent tubes (Gerstel). The first set was two tubes connected in parallel. One of these tubes was used to collect emissions during the cold-start phase of UC (the first 5 min, commonly referred to as bag 1), and the other tube was used to collect emissions during the combined hot-running and hot-start phases of the UC (bags 2 and 3). The second set of sorbent tubes was connected in series to collect emissions over the entire UC test. The total flow rate through filters was 47 slpm and 0.5 slpm through each Tenax tube. The sampling trains were housed in a heated enclosure (47 ± 5 °C) mimicking the CFR86 protocol.

Dynamic blanks were collected for both filters and adsorbent tubes when the CVS was operated only on dilution air (no vehicle exhaust) for the same period as the UC. Prior to sampling, the quartz filters were prefired at 550 °C in air for at least 12 h and Tenax adsorbent tubes were thermally regenerated at 320 °C in the helium flow to reduce their organic background. After sampling, the quartz filters and adsorbent tubes were stored at −24 °C until analysis. The blank levels for the sorbent tubes were consistently a small fraction of the sampled masses, at most 5% of the total mass and much less on a per compound basis. The quartz filter blanks were small enough in the SVOC range as to not affect the composition determination of the POA within measurement uncertainty.

VOC were analyzed using standard protocols as in previously published companion manuscripts.[15,21,38] Details are given in the Supporting Information.

Sorbent tubes and filters were analyzed using thermal desorption gas chromatography with mass spectrometry. Filters were subsampled for organic analysis using 0.4 cm^2 punches, spiked with internal standards (perdeuterated *n*-alkanes with even carbon numbers from C8−C34), loaded into a thermal desorption and autosampler system (TDS3 and TDSA2; Gerstel Inc.), and heated to 300 °C under helium flow to transfer to a liquid-nitrogen cooled inlet for cryo-focusing on a quartz wool inlet liner (CIS4, Gerstel, Inc.) at 0 °C. Sorbent tubes were heated to only 275 °C. Injection into the GC column was achieved by rapid heating of the cooled injection system (CIS) (10 °C s^{-1}) up to 320 °C under a flow of helium. Analytes were separated in two chromatographic dimensions (GC × GC) using an Agilent 7890 GC equipped with a nonpolar primary column (60 m × 0.25 mm × 250 μm Rxi-5Sil-MS, Restek) and a polar secondary column (1 m Rtx-200, Restek) at a flow rate of 2 mL min^{-1} helium. A thermal modulator (Zoex) with cryogenic focusing served as the interface between the primary and secondary columns, with a modulation period set at 2.3 s. The GC temperature program was 40 °C with a 5 min hold, 3.5 °C min^{-1} up to 320 °C, and a final hold at 320 °C for 10 min. Following GC separation, analytes were ionized using electron impact ionization (EI) or a vacuum-ultraviolet (VUV) photon beam at 10.5 eV.[40] Data were collected using a time-of-flight (ToF) mass spectrometer (TOFWERK). The ion source operated at 170 °C to minimize fragmentation with VUV ionization and 270 °C with EI ionization to better maintain volatilization of the GC effluent. The VUV photon flux of ~10^{16} photons $cm^{-2}{\cdot}s^{-1}$ was generated by the Chemical Dynamics Beamline 9.0.2 of the Advanced Light Source at the Lawrence Berkeley National Laboratory.

Quantification of IVOC and SVOC. The Tenax sorbent samples were quantified to determine IVOC emissions using electron impact ionization with methods similar to that used by Zhao et al., except being adapted for GC × GC methods.[9,22] IVOC material was classified into three categories: aliphatic, single ring aromatics (IVOC-SRA), and general IVOC (Gen-IVOC). Classification within these three classes of compounds was determined by differences in second dimension retention time (polarity space) and by mass spectral characteristics in our GC × GC-MS analysis (Figure S2). All three classes of compounds were quantified by either compound specific calibration using more than 80 known standards or relating total ion chromatogram (TIC) signals to calibration standards of similar volatility and polarity (Table S1). In GC × GC, the TIC signal corresponds to a blob, or region, in volatility and polarity retention space. These blobs are analogous to peaks in traditional single-dimension chromatography. The GC-Image software package was used to define blobs from 2D chromatograms. Compounds were quantified by relating their TIC signals to that of the nearest standard in terms of polarity and volatility. Naphthalene, 1-methyl naphthalene, and 2-methyl naphthalene were directly quantified as specific compounds. Volatility bins were defined which are evenly spaced with their center elution times corresponding to each *n*-alkane. IVOC-SRA mass was quantified using the nearest *n*-alkane and the relative sensitivities derived from available aromatic standards (Table S1). GEN-IVOC masses were quantified using the most similar, available polycyclic aromatic hydrocarbons (PAH) and polar compound standards.

The mass spectra of the TIC blobs for IVOC-SRA were further analyzed to gain information on their isomeric composition. The TIC chromatograms were decomposed into selected ion chromatograms (SIC) using fragments that characterize IVOC-SRA (*m*/*z* 57, 71, 77, 83, 91, 92, 105, 106, 117, 118, 119, 120, 131, 133, 134, 144, 145, 147, 148). Blobs were then generated from each SIC, and these single ion blobs were recombined to create new pseudo-TIC blobs that contained only these selected ions. This makes the original chromatograms much cleaner, and the mass spectra for the reconstructed pseudo-TIC blobs can be classified into one of several categories defined by the alkyl substituents attached to the benzene ring: linear, disubstituted, poly substituted, groups tertiary at the C1 position (e.g., isopropyl), unsaturated compounds (such as tetralins), and unclassified compounds that are identified as aromatic but do not fit into one of the other categories. The unclassified category may include compounds that coelute, such that blob decomposition does distinguish them. Diagnostic ratios of key mass fragment signals for categorization were derived from the mass spectra for all SRA compounds with between 11 and 16 carbons available in the NIST library.

The quartz filter samples (POA) were analyzed for SVOC emissions with GC-VUV-MS using methods for quantification on the basis of those developed by Worton et al., Isaacman et al., Chan et al., and recently Nowak et al.[6,24,40−42] The molecular ion signals for linear, branched, cyclic, and aromatic hydrocarbons under VUV ionization are used as the basis for quantification. Sensitivity of the molecular ion for any given compound is a function of its thermal transfer efficiency, ionization efficiency, and degree of fragmentation. Authentic standards of more than 80 compounds were used for calibration (Table S1). Further details on transfer efficiency, accounting for sensitivity to the number of double bond equivalencies, and standards are given in the Supporting Information.

DOI: 10.1021/acs.est.8b05600
Environ. Sci. Technol. XXXX, XXX, XXX−XXX

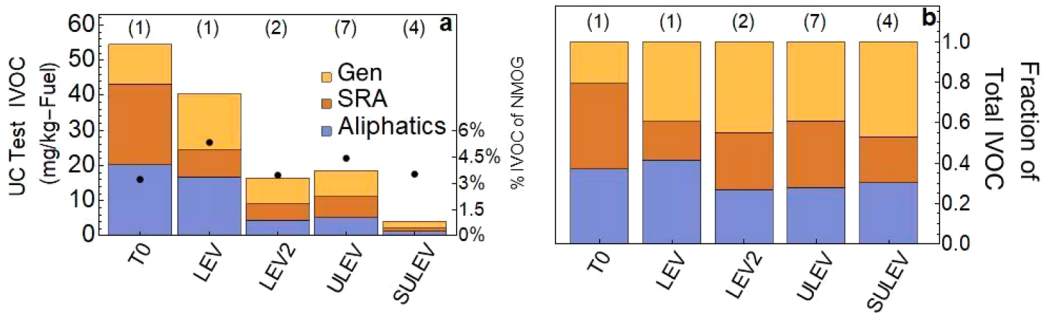

Figure 1. Average IVOC emissions for each vehicle class. (a) Aliphatic (blue), IVOC-SRA (brown), and Gen-IVOC (yellow). (b) Fractional composition of emissions. The number of vehicles included is noted above each class in parentheses. The black points in (a) show the percentage of IVOC in NMOG.

Engine Oil Analysis. Engine lubricating oil samples were taken for most vehicles and stored in sealed glass containers at −24 °C until analysis. Samples were diluted (50:1) in chloroform (Sigma-Aldrich, HPLC grade) and then directly injected into the heated GC inlet. The GC temperature program and column set was the same as above for IVOC and SVOC analysis. The quantification was nearly identical to the GC-VUV-MS analysis described above, except for the method of ionization, as detailed in Blair et al.[43] A soft electron-impact ion source (Markes Select-eV time-of-flight MS) was used as the ionization source.

Emission Factors. Pollutant data are reported as fuel-based emission factors (mass emitted per mass of fuel consumed) using a carbon mass balance approach

$$EF_i = \triangle m_i \frac{x_c}{\triangle CO_2 + \triangle CO + \triangle THC} \quad (1)$$

$\triangle CO_2$, $\triangle CO$, and $\triangle THC$ are the background-corrected concentrations of CO_2, CO, and THC. The fuel had a measured carbon mass fraction, x_c, of 0.82. $\triangle m_i$ is the measured background-corrected concentration of species i. Fuel consumption per mile data are presented in Saliba et al. and Drozd et al.[21,38]

RESULTS AND DISCUSSION

Total IVOC Emissions and Overall Composition. The total IVOC emissions collected on sorbent tubes for all vehicle classes are shown in Figure 1a, displayed as the average emission factors for all vehicles in each class. Complete composition data were available for the following gasoline vehicles: 4 (SULEV+PZEV), 5 ULEV, 2 LEV II, 1 Lev I, and 1 Tier 0. Emissions drop by about an order of magnitude from the vehicle with the least strict emission controls (Tier 0) to those with most advanced controls (SULEV). There is a drop of about a factor of 2 in IVOC emissions between the LEV I and LEV II vehicles, mirroring the decrease in NMOG emissions shown in companion publications.[21,38] Most of the NMOG emissions are VOCs, the main target for ozone controls. Figures 1 and S3 show that as NMOG emissions are reduced in response to stricter standards, IVOC emissions are reduced significantly as well, although the trend for the two classes of emissions is different. The IVOC emissions from the average SULEV vehicle are a factor of 10 lower than the T0vehicle; in contrast, the reduction in NMOG emissions was a factor of 40.[21] Therefore, it appears that the tightening of emission standards may not lead to the reduction of IVOC emissions as effectively as the reduction in total NMOG emissions.

Results for the IVOC composition are shown in Figure 1b. These emissions have been broadly grouped into three chemical classes: aliphatic, IVOC-SRA, and Gen-IVOC. The total IVOC composition does not vary significantly among the different vehicle classes. The aliphatic group is dominated by branched alkanes with 2% or less *n*-alkanes and cyclic alkanes. Aliphatic compounds are the most consistent fraction of IVOC emissions (35 ± 5%); this is higher than the previous estimate of Zhao et al. (20%).[22] Unlike the direct measurements presented here, the estimate of Zhao was based on traditional one-dimensional GC analysis that did not directly resolve the branched component of the aliphatic emissions. IVOC-SRA contribute 30 ± 10% of the total IVOC mass. IVOC-SRA include a number of alkyl benzene compounds with the alkyl substituents varying in the number of alkyl chains, rings, and branching. Gen-IVOC compounds contribute 35 ± 10% of IVOC. The Gen-IVOC category has high fractions of naphthalene and alkylated naphthalenes, with naphthalene and methylnaphthalenes contributing 60 ± 15% of total Gen-IVOC mass across all vehicle classes. Naphthalenes are 20 ± 5% of total IVOC emissions, consistent with the results of Zhao et al.[22] Importantly, we now identify the unspeciated "cyclic" compounds of Zhao et al.[22] as mainly IVOC-SRA, with cyclic aliphatic material contributing less than 1% of the IVOC emissions.

Volatility of IVOC Emissions. The volatility distribution of the IVOC emissions, expressed as carbon number for the equivalent *n*-alkane and $\log_{10}(C^*(\mu g\ m^{-3}))$, is shown in Figure S4. The bins span $\log_{10}(C^*)$ of 6 to 2.5, and each bin is further divided by molecular structure. Each panel shows the results from the average vehicle in each emissions standard group. All the IVOC distributions peak in the n12 or n13 bins ($\log_{10}(C^*)$ = 6 and 5.5, respectively). The n12 and n13 bins also contain the overwhelming majority of PAH and Gen-IVOC material, because naphthalene and the methyl naphthalenes fall in these bins. These compounds are in the lower range of volatility for gasoline fuels.[44] IVOCs emitted from gasoline vehicles with less advanced emission control technology have somewhat broader volatility distributions with more emissions in bins beyond n14. ULEV and SULEV vehicles both have distributions with over 90% of the IVOC emissions in the n12 and n13 bins. Our volatility distribution results are broadly consistent with the results of Zhao et al., who also found the majority of IVOC mass with volatilities similar to C12−C14 *n*-alkanes.[22]

DOI: 10.1021/acs.est.8b05600
Environ. Sci. Technol. XXXX, XXX, XXX−XXX

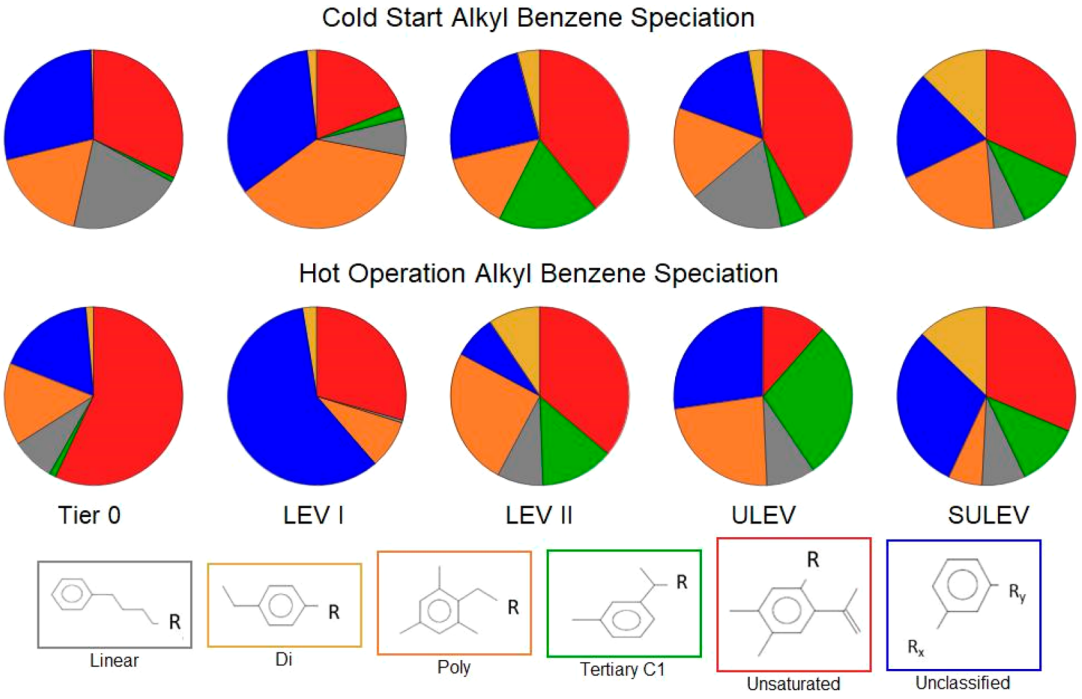

Figure 2. Classification of IVOC-SRA across all vehicle classes. Cold-start emissions are shown in the top panel; hot-operating emissions are shown in the bottom panel. The types of SRA are shown according to color: linear (gray), disubstituted (gold), poly substituted (orange), tertiary at C1 position (green), unsaturated (red), unclassified (blue). The structures are general so that they may vary by more than just the R group but also by position and number of R groups.

Characterization of IVOC-SRA. Emissions of SRA with fewer than 10 carbons are commonly measured, but much less is known about the composition of IVOC-SRA. As shown in Figure 1, IVOC-SRA comprise about 30 ± 10% of the total IVOC mass for all vehicle classes. Furthermore, IVOC-SRA have not been studied in smog chamber experiments but potentially have high SOA yields.[45−47] IVOC-SRA include alkyl benzenes with 5−12 carbons in addition to the basic benzene ring. We include in the SRA category compounds that have cyclic aliphatic segments, such as tetralins, because these have a single aromatic ring and elute with a similar retention time in our polarity separation as alkyl benzenes. Given that the number of potential isomers increases dramatically with the number of substituent carbons, these larger SRA can be difficult to separate and identify uniquely. As detailed in the methods section, we utilized the separation capability of GC × GC and diagnostic fragmentation in EI ionization to extensively characterize the SRA in the IVOC range.

The distribution of IVOC-SRA types for cold-starts and hot-operation from all vehicle classes are presented in Figure 2. IVOC-SRA emissions during both engine states (and for all emission control categories) have 30 ± 10% unsaturated compounds. This type of SRA is mainly composed of substituted tetralin and indane compounds. These compounds are of particular interest because little is known about their SOA formation potential; they are also known to be present in the lower volatility range of gasoline fuels.[44] Linear substituted species always contributed less than 25% of the total IVOC-SRA. We show here that the unspeciated cyclic compounds from Zhao et al. are dominated by aromatic species. Because of the diversity in IVOC-SRA structures and their potential for varying SOA yield, *n*-alkyl substituents are not likely to accurately represent SOA formation from the full suite of IVOC-SRA present in vehicle exhaust. There is not a clear trend in IVOC-SRA composition with vehicle emissions certification standards, and there is greater similarity between cold- and hot-operation IVOC-SRA compositions than that across vehicle class. Comparisons across class may be obscured by the sometimes large fraction of unclassified aromatics (blue), which could include compounds that are structurally similar to compounds in other IVOC-SRA categories. In addition, the test fleet is relatively small, and a larger fleet size might smooth out variability to give a clearer depiction of an average IVOC-SRA composition for each vehicle class. Given the results shown in Figure 1b, we believe that a larger fleet and improved classification would show IVOC-SRA compositions to be similar across vehicle classes.

Relationship between NMOG and IVOC Emissions. The ratio of IVOC emissions (GC × GC measurements) to NMOG emissions (heated FID measurements) can be used to estimate trends in IVOC emissions. Our results for the percentage of IVOC in NMOG are shown in Figure 1 and Figure S3. IVOC comprise 3.9 ± 1% of the NMOG emissions averaged over the full UC drive cycle, and there is no clear trend in this fraction with vehicle emissions class. Our estimate is in good agreement with that of Zhao et al., who used similar methods to estimate that IVOC are 4 ± 2% of NMOG emissions for a larger fleet of older vehicles (Pre-LEV to LEV II).[22] Gentner et al. and Schauer et al. estimated lower contributions of IVOC to NMOG of 1−2%.[23,26] Gentner's estimate was based on fuel analyses, while Schauer's was based on much older vehicles.

Cold-Start Effects on IVOC Emissions. Engine and aftertreatment condition strongly influence vehicle emissions.[4,21,22,48−50] Emission factors are typically much smaller during hot-operation compared to cold-start, because the catalytic converter has reached its light off temperature. The impact of engine state and aftertreatment on IVOC emissions

DOI: 10.1021/acs.est.8b05600
Environ. Sci. Technol. XXXX, XXX, XXX−XXX

is shown in Figure 3. The ratio of cold/hot IVOC emission factors is listed above each pair of data. Figure 3 indicates that

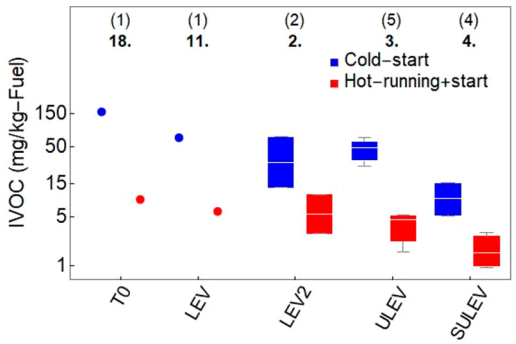

Figure 3. Comparison of IVOC emission factors for cold-start (blue) and combined hot-running and hot-start (red) for all vehicle classes. Number of vehicles included is shown above each class in parentheses, below which is listed the median ratio of cold/hot IVOC emissions for that class. Note the logarithmic *y*-axis scale for emissions.

the disparity between cold-start versus hot-operation emission factors has decreased for newer vehicles that meet stricter total emission standards. The oldest technology vehicle (T0) has cold-start emission factors that are 18× the hot-operation emission factors, while for the newest technology vehicles (SULEV), this ratio is 6. This indicates proportionally larger decreases in cold-start emission factors compared to hot-operation emission factors. The effectiveness of emission control systems has likely improved more for cold-starts than for hot-operation because of the incorporation of close-coupled catalytic converters.[8] Given that the high emitting vehicles in our fleet have lower than average IVOC emissions compared to previous studies, this trend, while warranting further study, is likely to be upheld for a larger fleet.[10,22,30]

The importance of the cold-start can also be expressed as the number of miles, γ, that must be driven for emissions of a given compound or class of compounds during hot-operation to equal the total mass of emissions during cold-start (UC bag 1). These results are presented in Figure S5. The fleet average γ is 18 ± 8 miles, ranging from 32 miles for the T0 vehicle to 11 miles for the SULEV vehicles. The average trip distance in the US is 10 miles,[38] so IVOC emissions from older vehicles are dominated by cold-starts. However, for newer vehicles, cold- and hot-operations contribute more equally to the IVOC emissions. These γ-values can be compared to other pollutants. Many pollutants (CO, NO_x, primary organic aerosol, black carbon) have γ-values less than 20 miles, similar to IVOCs for newer vehicles.[21,38] The γ-values for NMOG emissions range from about 10 to 200 miles and increase when moved from older (T0) to newer (SULEV) vehicles, in contrast to the γ-values for IVOCs that decrease for newer vehicles. This is shown in Figure S5, and was also seen by Zhao et al.[13,22] This difference in response of NMOG and IVOCs to emission controls suggests that the emissions of these two classes of pollutants are relatively less coupled with newer control technologies.

Characterization of Primary Organic Aerosol Emissions. We characterized the POA collected on bare quartz filters according to the degree of branching, number of cyclic rings, aromatic character, and carbon number. These results for each vehicle class are presented in Figure S6, along with the composition of used motor oil. The molecular composition of the POA is consistent with the engine lubricating oil sampled from the same vehicle. A recent study using this same analysis method also found that vehicle exhaust POA was dominated by lubricating oil.[24] The majority of the POA mass, 85% or more, is composed of double bond equivalency (DBE) classes 1−3, which comprises cyclic and polycyclic aliphatic material. Straight chain and branched linear compounds together typically contribute less than 10% of the total POA mass. The DBE 4+ class, including aromatic compounds and PAH, contributes the remaining 5%. This is much less than the IVOC emissions, which have roughly 30 ± 10% in SRA-IVOC alone.

The emission factors for POA vary less than the emission factors for IVOC, which causes the ratio of IVOC emission factor to POA emission factor to vary by vehicle class. For gasoline vehicles with less effective emission controls (T0 and LEV), the IVOC/POA ratio varies between 10 to 20 versus between 1 to 3 for vehicles with more effective emission controls (ULEV and SULEV). Recent work from Zhao et al. with a larger fleet found an IVOC/POA emission factor ratio of 6 ± 4, which is in between the values for the smaller fleet

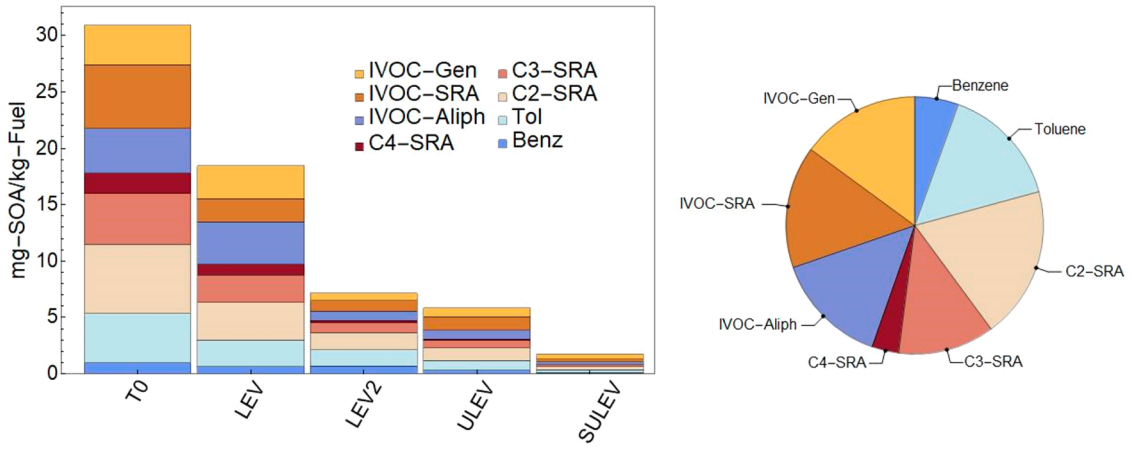

Figure 4. Potential SOA production from VOC-SRA and IVOC vehicular emissions for all vehicle classes. The chart on the left shows magnitude and composition for each class; the pie chart on the right shows the average compositions of emissions leading to potential SOA formation for all vehicle classes. We use an atmospheric OA level of 10 μg m^{-3} and oxidation of 24 h at an OH concentration of 1.5 × 10^6 molecules/cm^3.

DOI: 10.1021/acs.est.8b05600
Environ. Sci. Technol. XXXX, XXX, XXX−XXX

presented here.[22] The combined results of this study and that of Zhao et al. suggest that scaling factors applied to the POA emissions are not a robust strategy for estimating IVOC emissions, or at least show dependence on vehicle class.[16]

SOA Formation Potential. The detailed speciation of vehicle exhaust allows us to estimate the SOA formation potential for each vehicle class, as shown in Figure 4. We used published SOA yield parametrizations derived from smog chamber experiments for the VOC-SRA, with up to 10 carbons, and the three IVOC categories (aliphatic, IVOC-SRA, and Gen-IVOC). We performed the analysis under urban-like conditions with an atmospheric OA level of 10 μg m^{-3} and oxidation of 24 h at an OH concentration of 1.5 × 10^6 molecules/cm^3.[13,23,S1]

Mirroring the trends in absolute emissions, the predicted potential SOA formation decreases by an order of magnitude from the oldest control technology gasoline vehicle (T0, 32 mg-SOA/kg-fuel) to the newest control technologies (SULEV, 2 mg-SOA/kg-fuel). This range in SOA production is similar to that measured using a smog chamber with a slightly larger vehicle fleet (55 to 2 mg-SOA/kg-Fuel) and an oxidation flow reactor for the same vehicle fleet (55 to 5 mg-SOA/kg-Fuel).[13,15] This trend is expected because the decrease in the magnitudes of the identified SOA precursor emissions is also approximately a factor of 10 and the composition of emissions is consistent between vehicle classes.[13,21]

We predict that BTEX compounds (traditional aromatic SOA precursors) contribute to about 40% of SOA formation from gasoline vehicle emissions. IVOC compounds are predicted to contribute to 45% of SOA formation, and the remaining 15% of the predicted SOA is from VOC-SRA that are larger than BTEX compounds (but smaller than IVOCs). These results are in good agreement with estimates from Zhao et al, who also predicted that IVOCs contribute to about 50% of the SOA when assuming unspeciated cyclic compounds were aromatics.[22] IVOCs react faster than the smaller single ring VOC aromatics (e.g., benzene), so the ratio of SOA formed from IVOCs versus from VOC single ring aromatics changes with photochemical age, and at shorter ages IVOCs are relatively more important (Figure S7). For example, after 4 h of oxidation, BTEX compounds only contribute to 20% of the SOA, illustrating that BTEX compounds contribute a larger fraction to SOA formation as time increases. We show that oxidation of IVOC contributes to a significant fraction of SOA over a range of time scales and that larger aromatic compounds (IVOC-SRA and the majority of Gen-IVOC) contribute to two-thirds of the SOA from IVOCs.

Atmospheric Implications. Our detailed analysis of IVOC and SVOC emissions shows a similar composition across gasoline vehicles with varying emission control technologies. Consistency of exhaust composition is maintained despite a variation of a factor of 10 in the magnitude of emissions and differences in operating conditions (cold-start versus hot-operations). IVOC emissions occur throughout the entire UC test, with the highest emissions at cold-start but with less of an enhancement during cold-start compared to NMOG. Our more advanced analytical techniques reveal that the previously reported "cyclic" fraction of IVOC by Zhao et al.[22] is dominated by aromatics, and we continue the line of evidence showing that POA is composed of motor oil.

Our analysis of SOA formation potential indicates that IVOCs constitute an important class of SOA precursors in gasoline exhaust. The consistent compositions of the IVOC and SVOC exhaust emissions across many vehicle classes suggest that future reductions in the total emissions of organic gases, barring changes in atmospheric oxidation chemistry,[13] will continue to reduce SOA formation, consistent with Zhao et al.[13,15] Further study of oxidation and product formation from individual SRA-IVOC is needed to better determine the rate and magnitude of their SOA formation. The importance of IVOCs in SOA formation especially on short time scales (less 24 h) means that IVOC emissions need to be included in emission inventories and models.

■ ASSOCIATED CONTENT

Supporting Information

The Supporting Information is available free of charge on the ACS Publications website at DOI: 10.1021/acs.est.8b05600.

Figures showing sampling setup, example chromatogram, IVOC:NMOG correlations, volatility distributions, comparison of driving and cold-start emissions, POA composition, and time-dependent SOA formation. Tables of standards used, IVOC-SRA composition, and SOA yields and rate constants. (PDF)

■ AUTHOR INFORMATION

Corresponding Author

*E-mail: gtdrozd@colby.edu.

ORCID

Greg T. Drozd: 0000-0002-9195-6360
Yunliang Zhao: 0000-0002-9079-5972
Allen L. Robinson: 0000-0002-1819-083X

Notes

The authors declare no competing financial interest.

■ ACKNOWLEDGMENTS

We acknowledge the California Air Resources Board for funding (Contract No. 12-318).

■ REFERENCES

(1) Bahreini, R.; Middlebrook, A. M.; De Gouw, J. A.; Warneke, C.; Trainer, M.; Brock, C. A.; Stark, H.; Brown, S. S.; Dube, W. P.; Gilman, J. B.; et al. Gasoline Emissions Dominate over Diesel in Formation of Secondary Organic Aerosol Mass. *Geophys. Res. Lett.* **2012**, *39* (6), L06805.

(2) Mcdonald, B. C.; Gentner, D. R.; Goldstein, A. H.; Harley, R. a. Long-Term Trends in Motor Vehicle Emissions in U.S. Urban Areas. *Environ. Sci. Technol.* **2013**, *47* (17), 10022−10031.

(3) Jathar, S. H.; Gordon, T. D.; Hennigan, C. J.; Pye, H. O. T.; Pouliot, G.; Adams, P. J.; Donahue, N. M.; Robinson, A. L. Unspeciated Organic Emissions from Combustion Sources and Their Influence on the Secondary Organic Aerosol Budget in the United States. *Proc. Natl. Acad. Sci. U. S. A.* **2014**, *111* (29), 10473−10478.

(4) May, A. A.; Nguyen, N. T.; Presto, A. A.; Gordon, T. D.; Lipsky, E. M.; Karve, M.; Gutierrez, A.; Robertson, W. H.; Zhang, M.; Brandow, C.; et al. Gas- and Particle-Phase Primary Emissions from in-Use, on-Road Gasoline and Diesel Vehicles. *Atmos. Environ.* **2014**, *88*, 247−260.

(5) Gentner, D. R.; Jathar, S. H.; Gordon, T. D.; Bahreini, R.; Day, D. A.; El Haddad, I.; Hayes, P. L.; Pieber, S. M.; Platt, S. M.; de Gouw, J.; et al. Review of Urban Secondary Organic Aerosol Formation from Gasoline and Diesel Motor Vehicle Emissions. *Environ. Sci. Technol.* **2017**, *51*, 1074−1093.

(6) Chan, A. W. H.; Isaacman, G.; Wilson, K. R.; Worton, D. R.; Ruehl, C. R.; Nah, T.; Gentner, D. R.; Dallmann, T. R.; Kirchstetter, T. W.; Harley, R. A.; et al. Detailed Chemical Characterization of

DOI: 10.1021/acs.est.8b05600
Environ. Sci. Technol. XXXX, XXX, XXX−XXX

Unresolved Complex Mixtures in Atmospheric Organics: Insights into Emission Sources, Atmospheric Processing, and Secondary Organic Aerosol Formation. *J. Geophys. Res. Atmos.* **2013**, *118* (12), 6783−6796.
(7) Gentner, D. R.; Isaacman, G.; Worton, D. R.; Chan, A. W. H.; Dallmann, T. R.; Davis, L.; Liu, S.; Day, D. A.; Russell, L. M.; Wilson, K. R.; et al. Elucidating Secondary Organic Aerosol from Diesel and Gasoline Vehicles through Detailed Characterization of Organic Carbon Emissions. *Proc. Natl. Acad. Sci. U. S. A.* **2012**, *109* (45), 18318−18323.
(8) Frey, H. C. Trends in Onroad Transportation Energy and Emissions. *J. Air Waste Manage. Assoc.* **2018**, *68* (6), 514−563.
(9) Zhao, Y.; Nguyen, N. T.; Presto, A. A.; Hennigan, C. J.; May, A. A.; Robinson, A. L. Intermediate Volatility Organic Compound Emissions from On-Road Diesel Vehicles: Chemical Composition, Emission Factors, and Estimated Secondary Organic Aerosol Production. *Environ. Sci. Technol.* **2015**, *49*, 11516−11526.
(10) Gordon, T. D.; Tkacik, D. S.; Presto, A. A.; Zhang, M.; Jathar, S. H.; Nguyen, N. T.; Massetti, J.; Truong, T.; Cicero-Fernandez, P.; Maddox, C.; et al. Primary Gas- and Particle-Phase Emissions and Secondary Organic Aerosol Production from Gasoline and Diesel off-Road Engines. *Environ. Sci. Technol.* **2013**, *47* (24), 14137−14146.
(11) Platt, S. M.; El Haddad, I.; Zardini, A. A.; Clairotte, M.; Astorga, C.; Wolf, R.; Slowik, J. G.; Temime-Roussel, B.; Marchand, N.; Jezek, I.; et al. Secondary Organic Aerosol Formation from Gasoline Vehicle Emissions in a New Mobile Environmental Reaction Chamber. *Atmos. Chem. Phys.* **2013**, *13* (18), 9141−9158.
(12) Odum, J. R.; Hoffmann, T.; Bowman, F.; Collins, D.; Flagan, R. C.; Seinfeld, J. H. Gas/Particle Partitioning and Secondary Organic Aerosol Yields. *Environ. Sci. Technol.* **1996**, *30* (8), 2580−2585.
(13) Zhao, Y.; Saleh, R.; Saliba, G.; Presto, A. A.; Gordon, T. D.; Drozd, G. T.; Goldstein, A. H.; Donahue, N. M.; Robinson, A. L. Reducing Secondary Organic Aerosol Formation from Gasoline Vehicle Exhaust: Precursors and NOx Effects. *Proc. Natl. Acad. Sci. U. S. A.* **2017**, *114* (27), 6984−6989.
(14) Tkacik, D. S.; Presto, A. A.; Donahue, N. M.; Robinson, A. L. Secondary Organic Aerosol Formation from Intermediate-Volatility Organic Compounds: Cyclic, Linear, and Branched Alkanes. *Environ. Sci. Technol.* **2012**, *46* (16), 8773−8781.
(15) Zhao, Y.; Lambe, A. T.; Saleh, R.; Saliba, G.; Robinson, A. L. Secondary Organic Aerosol Production from Gasoline Vehicle Exhaust: Effects of Engine Technology, cold-start, and Emission Certification Standard. *Environ. Sci. Technol.* **2018**, *52* (3), 1253−1261.
(16) Robinson, A. L.; Donahue, N. M.; Shrivastava, M. K.; Weitkamp, E. A.; Sage, A. M.; Grieshop, A. P.; Lane, T. E.; Pierce, J. R.; Pandis, S. N. Rethinking Organic Aerosols: Semivolatile Emissions and Photochemical Aging. *Science (Washington, DC, U. S.)* **2007**, *315* (5816), 1259−1262.
(17) Presto, A. A.; Miracolo, M. A.; Kroll, J. H.; Worsnop, D. R.; Robinson, A. L.; Donahue, N. M. Intermediate-Volatility Organic Compounds: A Potential Source of Ambient Oxidized Organic Aerosol. *Environ. Sci. Technol.* **2009**, *43* (13), 4744−4749.
(18) Bruehlmann, S.; Forss, A.-M.; Steffen, D.; Heeb, N. V. Benzene: A Secondary Pollutant Formed in the Three-Way Catalyst. *Environ. Sci. Technol.* **2005**, *39* (1), 331−338.
(19) Heeb, N. V.; Forss, A. M.; Weilenmann, M. Pre- and Post-Catalyst-, Fuel-, Velocity- and Acceleration-Dependent Benzene Emission Data of Gasoline-Driven EURO-2 Passenger Cars and Light Duty Vehicles. *Atmos. Environ.* **2002**, *36* (30), 4745−4756.
(20) Schauer, J. J.; Kleeman, M. J.; Cass, G. R.; Simoneit, B. R. T. Measurement of Emissions from Air Pollution Sources. 2. C1 through C30 Organic Compounds from Medium Duty Diesel Trucks. *Environ. Sci. Technol.* **1999**, *33* (10), 1578−1587.
(21) Drozd, G. T.; Zhao, Y.; Saliba, G.; Frodin, B.; Maddox, C.; Weber, R. J.; Chang, M.-C. O.; Maldonado, H.; Sardar, S.; Robinson, A. L.; et al. Time Resolved Measurements of Speciated Tailpipe Emissions from Motor Vehicles: Trends with Emission Control Technology, cold-start Effects, and Speciation. *Environ. Sci. Technol.* **2016**, *50*, 13592−13599.
(22) Zhao, Y.; Nguyen, N. T.; Presto, A. A.; Hennigan, C. J.; May, A. A.; Robinson, A. L. Intermediate Volatility Organic Compound Emissions from On-Road Gasoline Vehicles and Small Off-Road Gasoline Engines. *Environ. Sci. Technol.* **2016**, *50*, 4554−4563.
(23) Gentner, D. R.; Isaacman, G.; Worton, D. R.; Chan, A. W. H.; Dallmann, T. R.; Davis, L.; Liu, S.; Day, D. A.; Russell, L. M.; Wilson, K. R.; et al. Elucidating Secondary Organic Aerosol from Diesel and Gasoline Vehicles through Detailed Characterization of Organic Carbon Emissions. *Proc. Natl. Acad. Sci. U. S. A.* **2012**, *109* (45), 18318−18323.
(24) Worton, D. R.; Isaacman, G.; Gentner, D. R.; Dallmann, T. R.; Chan, A. W. H.; Ruehl, C.; Kirchstetter, T. W.; Wilson, K. R.; Harley, R. A.; Goldstein, A. H. Lubricating Oil Dominates Primary Organic Aerosol Emissions from Motor Vehicles. *Environ. Sci. Technol.* **2014**, *48* (7), 3698−3706.
(25) Kleeman, M. J.; Riddle, S. G.; Robert, M. a; Jakober, C. a. Lubricating Oil and Fuel Contributions to Particulate Matter Emissions from Light-Duty Gasoline and Heavy-Duty Diesel Vehicles. *Environ. Sci. Technol.* **2008**, *42* (1), 235−242.
(26) Schauer, J. J.; Kleeman, M. J.; Cass, G. R.; Simoneit, B. R. T. Measurement of Emissions from Air Pollution Sources. 5. C1-C32 Organic Compounds from Gasoline-Powered Motor Vehicles. *Environ. Sci. Technol.* **2002**, *36* (6), 1169−1180.
(27) Lim, Y. B.; Ziemann, P. J. Effects of Molecular Structure on Aerosol Yields from OH Radical-Initiated Reactions of Linear, Branched, and Cyclic Alkanes in the Presence of NOx. *Environ. Sci. Technol.* **2009**, *43* (7), 2328−2334.
(28) Jathar, S. H.; Miracolo, M. A.; Presto, A. A.; Donahue, N. M.; Adams, P. J.; Robinson, A. L. Modeling the Formation and Properties of Traditional and Non-Traditional Secondary Organic Aerosol: Problem Formulation and Application to Aircraft Exhaust. *Atmos. Chem. Phys.* **2012**, *12* (19), 9025−9040.
(29) Robinson, A. L.; Donahue, N. M.; Shrivastava, M. K.; Weitkamp, E. a; Sage, A. M.; Grieshop, A. P.; Lane, T. E.; Pierce, J. R.; Pandis, S. N. Rethinking Organic Aerosols. *Science (Washington, DC, U. S.)* **2007**, *315*, 1259−1262.
(30) May, A. A.; Presto, A. A.; Hennigan, C. J.; Nguyen, N. T.; Gordon, T. D.; Robinson, A. L. Gas-Particle Partitioning of Primary Organic Aerosol Emissions: (1) Gasoline Vehicle Exhaust. *Atmos. Environ.* **2013**, *77*, 128−139.
(31) Warneke, C.; De Gouw, J. A.; Holloway, J. S.; Peischl, J.; Ryerson, T. B.; Atlas, E.; Blake, D.; Trainer, M.; Parrish, D. D. Multiyear Trends in Volatile Organic Compounds in Los Angeles, California: Five Decades of Decreasing Emissions. *J. Geophys. Res. Atmos.* **2012**, *117* (D21), 1−10.
(32) Gordon, T. D.; Presto, A. A.; Nguyen, N. T.; Robertson, W. H.; Na, K.; Sahay, K. N.; Zhang, M.; Maddox, C.; Rieger, P.; Chattopadhyay, S.; et al. Secondary Organic Aerosol Production from Diesel Vehicle Exhaust: Impact of Aftertreatment, Fuel Chemistry and Driving Cycle. *Atmos. Chem. Phys.* **2014**, *14* (9), 4643−4659.
(33) Ng, N. L.; Chhabra, P. S.; Chan, A. W. H.; Surratt, J. D.; Kroll, J. H.; Kwan, A. J.; McCabe, D. C.; Wennberg, P. O.; Sorooshian, A.; Murphy, S. M.; et al. Effect of NOx Level on Secondary Organic Aerosol (SOA) Formation from the Photooxidation of Terpenes. *Atmos. Chem. Phys.* **2007**, *7* (19), 5159−5174.
(34) Liu, T.; Wang, X.; Deng, W.; Hu, Q.; Ding, X.; Zhang, Y.; He, Q.; Zhang, Z.; Lü, S.; Bi, X.; et al. Secondary Organic Aerosol Formation from Photochemical Aging of Light-Duty Gasoline Vehicle Exhausts in a Smog Chamber. *Atmos. Chem. Phys.* **2015**, *15* (15), 9049−9062.
(35) Nordin, E. Z.; Eriksson, A. C.; Roldin, P.; Nilsson, P. T.; Carlsson, J. E.; Kajos, M. K.; Hellén, H.; Wittbom, C.; Rissler, J.; Löndahl, J.; et al. Secondary Organic Aerosol Formation from Idling Gasoline Passenger Vehicle Emissions Investigated in a Smog Chamber. *Atmos. Chem. Phys.* **2013**, *13* (12), 6101−6116.

DOI: 10.1021/acs.est.8b05600
Environ. Sci. Technol. XXXX, XXX, XXX−XXX

(36) Jordan, C. E.; Ziemann, P. J.; Griffin, R. J.; Lim, Y. B.; Atkinson, R.; Arey, J. Modeling SOA Formation from OH Reactions with C8−C17 n-Alkanes. *Atmos. Environ.* **2008**, *42* (34), 8015−8026.
(37) Zhao, Y.; Hennigan, C. J.; May, A. A.; Tkacik, D. S.; De Gouw, J. A.; Gilman, J. B.; Kuster, W. C.; Borbon, A.; Robinson, A. L. Intermediate-Volatility Organic Compounds: A Large Source of Secondary Organic Aerosol. *Environ. Sci. Technol.* **2014**, *48* (23), 13743−13750.
(38) Saliba, G.; Saleh, R.; Zhao, Y.; Presto, A. A.; Lambe, A. T.; Frodin, B.; Sardar, S.; Maldonado, H.; Maddox, C.; May, A. A.; et al. Comparison of Gasoline Direct-Injection (GDI) and Port Fuel Injection (PFI) Vehicle Emissions: Emission Certification Standards, Cold-Start, Secondary Organic Aerosol Formation Potential, and Potential Climate Impacts. *Environ. Sci. Technol.* **2017**, *51* (11), 6542−6552.
(39) Pang, Y.; Fuentes, M.; Rieger, P. Trends in Selected Ambient Volatile Organic Compound (VOC) Concentrations and a Comparison to Mobile Source Emission Trends in California's South Coast Air Basin. *Atmos. Environ.* **2015**, *122*, 686−695.
(40) Isaacman, G.; Wilson, K. R.; Chan, A. W. H.; Worton, D. R.; Kimmel, J. R.; Nah, T.; Hohaus, T.; Gonin, M.; Kroll, J. H.; Worsnop, D. R.; et al. Improved Resolution of Hydrocarbon Structures and Constitutional Isomers in Complex Mixtures Using Gas Chromatography-Vacuum Ultraviolet-Mass Spectrometry. *Anal. Chem.* **2012**, *84* (5), 2335−2342.
(41) Nowak, J. A.; Shrestha, P. M.; Weber, R. J.; McKenna, A. M.; Chen, H.; Coates, J. D.; Goldstein, A. H. Comprehensive Analysis of Changes in Crude Oil Chemical Composition during Biosouring and Treatments. *Environ. Sci. Technol.* **2018**, *52* (3), 1290−1300.
(42) Nowak, J. A.; Weber, R. J.; Goldstein, A. H. Quantification of Isomerically Summed Hydrocarbon Contributions to Crude Oil by Carbon Number, Double Bond Equivalent, and Aromaticity Using Gas Chromatography with Tunable Vacuum Ultraviolet Ionization. *Analyst* **2018**, *143* (6), 1396−1405.
(43) Blair, S. L.; MacMillan, A. C.; Drozd, G. T.; Goldstein, A. H.; Chu, R. K.; Paša-Tolić, L.; Shaw, J. B.; Tolić, N.; Lin, P.; Laskin, J.; et al. Molecular Characterization of Organosulfur Compounds in Biodiesel and Diesel Fuel Secondary Organic Aerosol. *Environ. Sci. Technol.* **2017**, *51*, 119−127.
(44) Gentner, D. R.; Worton, D. R.; Isaacman, G.; Davis, L. C.; Dallmann, T. R.; Wood, E. C.; Herndon, S. C.; Goldstein, A. H.; Harley, R. A. Chemical Composition of Gas-Phase Organic Carbon Emissions from Motor Vehicles and Implications for Ozone Production. *Environ. Sci. Technol.* **2013**, *47*, 11837−11848.
(45) Na, K.; Song, C.; Cocker, D. R. Formation of Secondary Organic Aerosol from the Reaction of Styrene with Ozone in the Presence and Absence of Ammonia and Water. *Atmos. Environ.* **2006**, *40* (10), 1889−1900.
(46) Li, L.; Tang, P.; Nakao, S.; Kacarab, M.; Cocker, D. R. Novel Approach for Evaluating Secondary Organic Aerosol from Aromatic Hydrocarbons: Unified Method for Predicting Aerosol Composition and Formation. *Environ. Sci. Technol.* **2016**, *50* (12), 6249−6256.
(47) Li, L.; Tang, P.; Nakao, S.; Cocker, D. R. R., III Impact of Molecular Structure on Secondary Organic Aerosol Formation from Aromatic Hydrocarbon Photooxidation under Low NO x Conditions. *Atmos. Chem. Phys.* **2016**, *16*, 10793−10808.
(48) George, I. J.; Hays, M. D.; Herrington, J. S.; Preston, W.; Snow, R.; Faircloth, J.; George, B. J.; Long, T.; Baldauf, R. W. Effects of Cold Temperature and Ethanol Content on VOC Emissions from Light-Duty Gasoline Vehicles. *Environ. Sci. Technol.* **2015**, *49* (21), 13067−13074.
(49) Heeb, N. Velocity-Dependent Emission Factors of Benzene, Toluene and C2-Benzenes of a Passenger Car Equipped with and without a Regulated 3-Way Catalyst. *Atmos. Environ.* **2000**, *34* (7), 1123−1137.
(50) Heeb, N. V.; Forss, A. M.; Saxer, C. J.; Wilhelm, P. Methane, Benzene and Alkyl Benzene cold-start Emission Data of Gasoline-Driven Passenger Cars Representing the Vehicle Technology of the Last Two Decades. *Atmos. Environ.* **2003**, *37* (37), 5185−5195.
(51) Drozd, G. T.; Worton, D. R.; Aeppli, C.; Reddy, C. M.; Zhang, H.; Variano, E.; Goldstein, A. H. Modeling Comprehensive Chemical Composition of Weathered Oil Following a Marine Spill to Predict Ozone and Potential Secondary Aerosol Formation and Constrain Transport Pathways. *J. Geophys. Res. Ocean.* **2015**, *120* (11), 7300−7315.

DOI: 10.1021/acs.est.8b05600
Environ. Sci. Technol. XXXX, XXX, XXX−XXX